A STUDY OF PRESSURE AND FLOW IN A POPPET VALVE MODEL

SUBMITTED IN PARTIAL FULFILLMENT OF THE REQUIREMENTS FOR THE DEGREE OF

BACHELOR OF SCIENCE

at the

MASSACHUSETTS INSTITUTE OF TECHNOLOGY

(1954)

Signature redacted

Signature of Author .....

Signature redacted

Department of Mechanical Engineering

Department of Mechanical Engineering
Massachusetts Institute of Technology
Cambridge 39, Mass.
May 24, 1954

Professor Leicester P. Hamilton
Secretary of the Faculty
Massachusetts Institute of Technology
Cambridge 39, Massachusetts

Dear Professor Hamilton:

This thesis entitled "A Study of Pressure and Flow in a Poppet Valve Model" is submitted in partial fulfillment of the requirements for the degree of Bachelor of Science in Mechanical Engineering.

Respectfully submitted,

Manfred Tidor

Abstract

The pressure and flow in a poppet valve was studied by means of a large-scale, two dimensional, glass-sided model. Reynold number was used to establish dynamic similitude between the valve and the model. Air injection into the oil stream was used to chart streamlines, which were observed through the glass faces.

The results of the investigation were:

1. A high degree of vorticity is present downstream of the valve seat.
2. No hysteresis exists in the valve between increasing and decreasing flow.
3. A general thickening of the boundary layer occurs in the region just upstream of the seat.
4. A low-pressure area exists just inside the valve seat resulting in a pressure rise across the seat.
5. Turbulence exists in the seat region as observed by the dispersion of the air bubbles emanating from the seat.
6. The upstream pressure on the poppet face is almost constant along the face, decreasing by 10% up to the entrance of the seat. The pressure near the upstream end of the poppet face agrees within 1% with the inlet pressure

Introduction

Object of the Investigation

There frequently occurs in the operation of poppet-type relief valves a condition of instability resulting in oscillation of the poppet. This oscillation causes malfunctioning of the valve by deforming the seat under impact, subsequently leading to leakage.

As a small part into the investigation into valve instability and for purposes of learning more about valve design, this thesis was conducted to study the steady-state pressure and flow conditions in a poppet valve by means of a large scale model.

An attempt is made to obtain dimensionless curves for the flow in the valve model. Various pressures on the face of the poppet are determined and the flow pattern is studied.

The possibility of the preserve of a hysteresis between increasing and decreasing flow is investigated.

Acknowledgements

Many thanks are expressed to the Pantex Corporation for the grant which financed this project and for their continued interest during the investigation; to Professors Lowen Shearer and Gerhard Reethof for guidance in setting up the problem and carrying out the investigation; to Professor T.Y. Toong for his aid in interpreting the results; to the Dynamic Analysis and Control Laboratory for the loan of equipment and aid in procurement of materials; to Mr. Joseph Pressner, Miss Frances Fishman and Mrs. Shirley Hasson for their secretarial services.

Table of Contents

Preliminary Analysis

It is desired to reproduce the range of pressure and flow found in an actual valve. For this purpose, a Reynold number is used for dynamic similitude.

$$Re_{(v)} = \frac{VD}{\nu} = \frac{QD}{A\nu} = Re_{(m)}$$

where Re_v - Reynold number in actual valve

Re_m - Reynold number in model

V - Average velocity of flow in valve seat region: (ft/sec)

ν - kinematic viscosity (ft^2/sec)

Q_m, Q_v - flow rate (cfs)

D - hydraulic diameter (ft)

P - perimeter of flow cross-section (ft) using a hydraulic radius for rectangular ducts:

$$D = \frac{4A}{P}$$

where A - area of flow cross-section at seat (ft^2)

then

$$Re_{(v)} = \frac{4Q_v}{P_v\nu} \quad ; \quad Re_{(m)} = \frac{4Q_m}{P_m\nu}$$

If it is assumed that for small valve openings all the pressure drop occurs along the valve seat and that the flow in the seat region is fully developed laminar flow, it is possible to apply an equation for steady flow between stationary flat plates to determine the relation between pressure drop across the valve and the flow rate.[1]

1. Footmote: "Fluid Power Control" M.I.T. Department of Mechanical Engineering.

$$\frac{\Delta P}{S} = \frac{12 \mu Q}{w h^3} \quad 1.$$

S_m, S_v - seat width (in.)

μ - viscosity (lb sec/ft^2)

h_m, h_v - valve opening (in.)

Δp - pressure drop across the valve seat (lb/ft^2)

wh - area of flow cross-section.

For the actual valve:

wh - $\pi d h_v$

d - diameter of seat in valve. (in.)

For the model:

wh = 1 x h (in.^{2})

Therefore

$$Re_v = \frac{2 \Delta P_v h_v^3}{(12)^4 \mu S_m \nu}$$

$$Re_m = \frac{2 \Delta P_m h_m^3}{(12)^4 \mu S_m \nu (1+h_m}$$

for small valve openings $1 + h_m \approx 1$

Equating the two Reynold numbers:

$$\frac{\Delta P_v}{\Delta P_m} = \frac{S_v h_m 3}{S_m h_v 3}$$

For geometric similitude the ratios $\frac{h_m}{h_v}$ and $\frac{S_m}{S_v}$ must be the same. Using β to denote the scale factor $\frac{h_m}{h_v}$ (or $\frac{S_m}{S_v}$) :

$$\frac{\Delta P_v}{\Delta P_m} = \beta^2$$

For large valve openings, ($^h/_s = 1$), it is assumed that the flow through the valve will resemble orifice flow, with an orifice coeficient, C, the flow rates through the valve and the model may be represented by:

$$Q_v = \frac{C \times \pi d h_v}{144} \sqrt{\frac{2}{\rho}(\Delta p_v)}$$

and

$$Q_m = \frac{C \times h_m}{144} \sqrt{\frac{2}{\rho}(\Delta p_m)}$$

then

$$Re_v = \frac{C \times 2 h_v}{144 \nu} \sqrt{\frac{2}{\rho}(\Delta p_v)}$$

and

$$Re_m = \frac{C \times 2 h_m}{144 \nu} \sqrt{\frac{2}{\rho}(\Delta p_m)} \qquad \text{for } h_m << 1$$

Equating Reynold numbers as before:

$$\frac{C \times 2 h_v}{144 \nu} \sqrt{\frac{2}{\rho}(\Delta p_v)} = \frac{C \times 2 h_m}{144 \nu} \sqrt{\frac{2}{\rho}(\Delta p_m)}$$

$$\frac{\Delta p_v}{\Delta p_m} = \frac{h_m^2}{h_v^2} = \beta^2$$

The same scale factor, β, applies to both laminar and orifice flow.

The maximum pressure controlled by the actual valve is 4000 pounds per square inch. The maximum pressure in the model should not exceed 40 pounds per square inch to prevent fracture of the glass faces.

$$\frac{\Delta p_v}{\Delta p_m} = \beta^2 = \frac{4000}{40} = 100 \qquad ; \quad \beta = 10$$

The full range of operation of the actual valve may be reproduced in a two-dimensional model of unit thickness with dimensions scaled up ten times from the valve.

A scale factor of only ten, however, does not provide a large enough seat width to insert pressure taps on the seat face for the study of pressures

along the seat. The lapped seat of a poppet valve can vary in width anywhere from .001 inch to .01 inch. Assuming a seat width of .006 inch in the valve, the model would have a seat width of only .06 inch with a scale factor of 10. With a scale factor of 20, the seat width on the model becomes .12 inch providing enough space for the location of three pressure taps along the seat face.

The main reason for limiting the scale factor to 20 is that the glass faces, which were borrowed from Dr. S. Y. Lee, were of a size to accommodate a model only 20 times the size of the actual valve.

The symmetry of the flow channel in the valve about the axis of the poppet shaft permits the use of only half the poppet for a complete study of the pressure and flow in the valve.

Flow coefficients

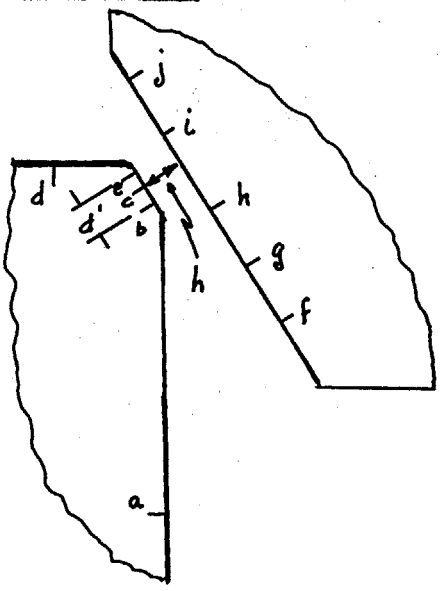

Figure 1

If the flow in the converging region is considered to fill the whole seat cross-section (h), a flow coefficient relating the actual flow (Qc) through the model to the expected flow (Qi) according to Bernoulli's equation for non-viscous, incompressible flow between points a and b (fig. 1) can be used to give an indication of contraction of the flow at the seat and any unusual changes in the flow as it bends to enter the seat region.

Bernoulli's equation:

$$\frac{V_b^2 - V_a^2}{2} = \frac{P_a - P_b}{\rho}$$

From the equation of continuity

$$V_a^2 = \left(\frac{A_b}{A_a}\right)^2 V_b^2$$

where A_a - area of flow cross-section at a (ft^2)

A_b - area of flow cross-section at b (ft^2)

Then

$$\frac{V_b^2}{2}\left[1 - \left(\frac{A_b}{A_a}\right)^2\right] = \frac{P_a - P_b}{\rho}$$

or

$$V_b = \sqrt{\frac{2}{\rho}\frac{(P_a - P_b)}{\left[1 - \left(\frac{A_b}{A_a}\right)^2\right]}}$$

Since A_a is always much greater than A_b (see Assembly drawing in Appendix III)

$$\left[1 - \left(\frac{A_b}{A_a}\right)^2\right] \approx 1$$

The flow $Q_i = A_b V_b$

where $A_b = \frac{hm}{144}$

and

$$Q_i = \sqrt{\frac{2}{\rho}(P_a - P_b)}\ \frac{hm}{144}$$

The flow coefficient, C, is defined as:

$$C = \frac{Qc}{Qi} = \frac{Q_c}{\frac{h_m}{144}\sqrt{\frac{2}{\rho}(p_a - p_b)}}$$

Another flow coefficient, K, may be used to relate the measured flow in the seat region to the fully-developed laminar flow which would exist between stationary flat plates with the same pressure drop from b to e (fig. 1)

The expression for fully developed laminar flow between flat one-inch plates of separation, h_m, with a pressure drop, ΔP, along a length d is:

$$Q_e = \frac{h_m^3 \Delta P_m}{(12)^2 \mu d}$$

where Q_e - flow rate (ft^3/sec)

ΔP - pressure drop (psf)

d - distance between points b and e (ft)

The flow coefficient, K, is expressed as:

$$K = \frac{Qc}{Qe} = \frac{Qc}{h_m^3 \Delta P_m / 12 \mu d}$$

The change in K with valve opening and increasing flow rate gives an indication of the relation of the actual flow to fully developed laminar flow and serves as an aid in analyzing the flow conditions in the seat region of the model.

After a few calculations of K, this method of analysis was abandoned. It became apparent that there was no relation between the actual flow in the seat region and fully-developed laminar flow.

To complete the design of the valve model, it is necessary to determine the number and position of the required pressure taps. Over all pressure drop across the valve model is defined between points a and d (Fig. 1)

Five pressure taps are to be distributed along the poppet face to determine the pressure pattern on the poppet. Three pressure taps are located along the valve seat for the calculation of flow coefficients and to observe the pressure pattern along the seat.

The values to be measured in this investigation are pressures at the various taps, oil flow rate through the model, and temperature of the oil for the determination of density and kinematic viscosity.

Several methods of pressure measurement were investigated including Bourdon pressure gages, strain gages fastened to diaphragms and mercury manometers. Bourdon pressure gages were eliminated for their low sensitivity, lack of sufficient number available around the Institute and their high purchase price.

Strain gage pressure cells were not thought feasible because of the necessity of calibrating each one individually and because of the long time interval which would be required to read a complete set of the ten pressure values.

The manometer board was decided upon, because

it is relatively inexpensive to build and provides a method of visual comparison, at a single glance, of all the pressures in the valve at a given flow and opening.

The flowmeter is described under the section "The test set-up". The oil temperature is obtained from a gage which reads the oil temperature in the sump.

In plotting the pressure-flow curves for the valve, a Reynold number is used to denote dimensionless flow and the ratio of pressure drop to inlet pressure is used to denote dimensionless pressure. Two Reynold numbers are considered, One as a function of seat width ($\frac{Vs}{\nu}$), the other, as a function of valve opening ($\frac{Vh}{\nu}$). Subsequent plotting of the data using both Reynold numbers, indicated a single curve may be used to represent the flow in the valve at all openings using the Reynold number as a function of opening ($R_e = \frac{Vh}{\nu}$)

The test Set-up

a) The valve model (See Appendix III)

For purposes of correlation with existing valve design, the valve configuration used for this investigation was a two-dimensional enlarged version of the pilot stage of the Pantex ½ inch relief valve, model number AA 8-06 manufactured by the Pantex Manufacturing Corporation of Pawtucket, Rhode Island. An approximate enlargement factor of 20 was used.

The top and bottom surfaces of the valve model were made of one-inch plate glass to make possible visual observation of streamlines traced by air bubbles injected into the stream. Special bolts with oversized heads fastened the glass to the metal frame. (Fig. 2)

The seat and poppet were so designed as to be removable, with the intention of investigating several different poppet angles and shapes.

The pressure taps in the valve were designed with a .030 inch diameter so as to interfere as little as possible with the flow. This seemed particularly important in the seat region where three taps are located along a 1/8 inch width in an attempt to measure minute pressure changes across the seat face.

To minimize the time required for the stabilization of flow between the valve and the plastic tubing leading to the manometer, a tubing was needed with an outside diameter no larger than the inside

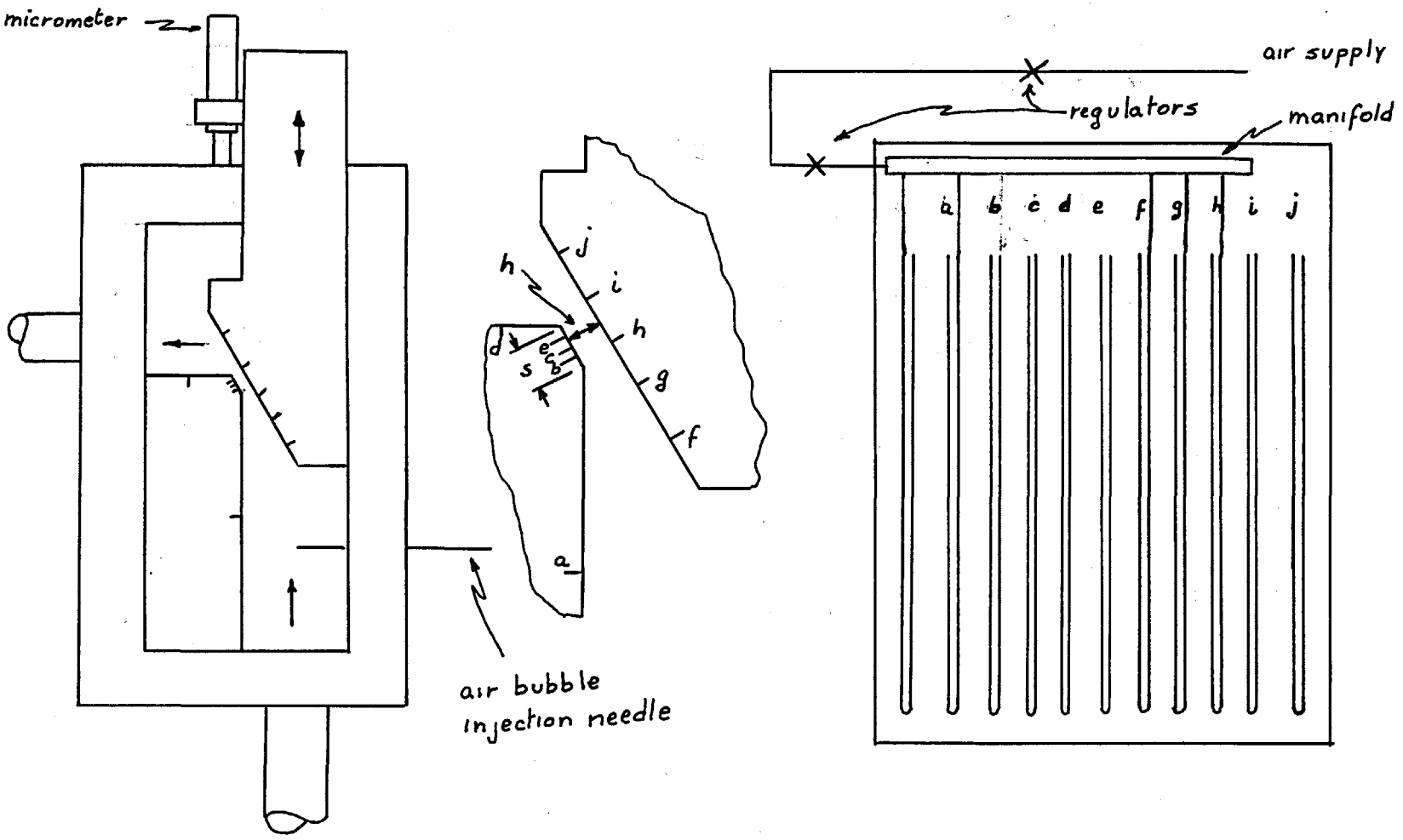

Valve model

Manometer board

Figure 2

diameter of the plastic tube and with as large an inside diameter as possible. The Procurement Division of the Dynamic Analysis and Control Laboratory managed to locate some nickel tubing with an outside diameter of .067 inches and an inside diameter of .048 inches.

Positioning of the poppet is accomplished by means of a micrometer spindle attached to the poppet outside of the valve frame. Since the poppet angle is 30° with the poppet axis, the reading of the micrometer is twice the valve opening. In this manner, valve openings in the model can be set with an accuracy better than .0005 inches. (Fig. 2).

Two holes are drilled in the valve frame, one on either side of the seat to be used for injecting air into the flow stream.

After an initial test, it became evident that the clamping friction of the glass was not sufficient to prevent the parts of the model from separating under internal oil pressure. Two U clamps were devised to clamp the metal parts of the valve together. (See photograph of valve model). Besides holding the model together against oil pressure, the clamps served to prevent the poppet from slipping once the proper valve opening was set.

In order to provide as uniform a flow as possible, 18 inch lengths of smooth-bored 7/8 inch steel tubes were soldered into the entrance and

exit ports. To prevent turbulence caused by a sudden increase in flow cross-section from the tube to the model, the entrance and exit ports were flared.

b) The manometer board

After attempting unsuccessfully to borrow the necessary manometers, it became imperative to build a U tube manometer board for this investigation.

In an effort to attain the optimum relation between ease of reading and maximum pressure range, a manometer length of four feet is used. To make possible the reading of higher pressures, a pressure manifold is attached to the manometer board and connected to the atmospheric end of the four manometers reading the pressures upstream of the valve seat. An extra manometer is added to the board to read the pressure in the manifold. This brings the total number of manometers on the board to eleven.

It was found necessary to add a low-pressure regulator in addition to the regulator in the air supply line to maintain a constant pressure in the manifold. Fluctuations in the regulated pressure were found to exist when only the high-pressure regulator in the air supply line was used.

The addition of the manifold doubles the range of the manometer. With mercury as a working fluid, the maximum pressure range is eight feet of mercury or about 45 psi.

A 1/8 inch multistrand plastic tubing is used to transmit the oil pressure from the valve model to the manometer board. A reduction coupling between the ¼ inch glass manometer and the 1/8 inch plastic tubing is made with seran tubing, ¼ inch copper tubing and 1/8 inch steel tubing.

First efforts in forcing the seran tubing onto the glass manometer resulted in a leaky coupling and in several attempts--broken glass. On the advice of lab technicians, the seran was heated before being forced over the glass. Care has to be taken in the heating as the seran is inflammable. A glue is used to further seal the connection and a hose clamp is applied while the seran is still soft. The stranded plastic tubing is forced over the other end of the coupling.

In the interest of keeping the front of the manometer board as uncluttered as possible, the multistrand tubing is brought in from the rear of the board through a hole over one leg of each manometer.

A heavy-duty paper scaled in tenths of an inch is fixed to the face of the board before the manometers are mounted; with this scale, pressure readings to the nearest .05 inch of mercury are possible.

Removing air from the lines leading to the manometer proved to be quite a problem. It was finally accomplished by a combination of cyclic application of pressure first on the atmospheric

leg of the manometer, then on the valve end of the pressure tubes; and hanging the plastic tubes vertically to cause the bubbles to rise to the surface of the oil.

The position of the valve model above the zero level of the manometer is noted for correction of recorded pressure for the differential oil pressure between the model and the surface of the mercury.

c) Air-bubble injection apparatus

In order to obtain a fine stream of air for good definition and to cause as little disturbance in the oil flow as possible, two hypodermic needles are used - one embedded in the tip of the other. The larger needle (.028D) is soldered into a hole drilled into a $\frac{1}{4}$ inch nut. A very short length - about 1/8 inch of the smaller needle (.012D) is soldered into the tip of the larger needle.

The $\frac{1}{4}$ inch nut is attached through a flexible 1/8 inch copper tube to a $\frac{1}{4}$ inch needle valve which is connected through a T to a small air cylinder. The other end of the T contains a bicycle valve for charging the tank.

The purpose of the extremely fine air stream obtained with this apparatus is to take pictures of the complete flow pattern by multiple exposures with a camera. With a fine air stream, the possibility of good definition close to the seat is increased.

A Polaroid camera mounted on an attachment

to take pictures on an oscilloscope is placed vertically on the upper glass face of the model. Lighting consists of a photoflood lamp located on either side of the model. A shiny surface is placed under the model to reflect the light upward into the oil.

The method used proved to be a failure. The high intensity of ambient light tended to fog the film before the light passing through the oil had a chance to register.

d) The flow meter

The flow meter used for this investigation consisted of a hydraulic motor geared to a tachometer whose electrical output was connected to a milliammeter.

Since part of this investigation consisted of checking for hysteresis in the flow, it was necessary to check for hysteresis in the flow meter. This was accomplished with a graduated cylinder and a stopwatch. The measurements indicated no hysteresis in the flow meter while cycling the flow.

Calibration of the flow meter was accomplished during the measurements for hysteresis.

e) The test stand

A Bendix hydraulic pump unit was used to provide the necessary pressures and flow. The oil used was an Esso Univis 40. (Variation of density and Kinematic viscosity with temperature given in Appendix IV)

Ordinarily the return line to the sump passes through a series of filters and a heat exchanger. The resistance of these elements to the passage of the oil would raise the pressure in the model beyond the safe load for the glass faces. It was found necessary to bypass both the heat exchangers and the filter by means of a two-inch rubber hose fed directly into the sump. This arrangement presented problems of overheating of the oil and necessitated frequent cooling periods.

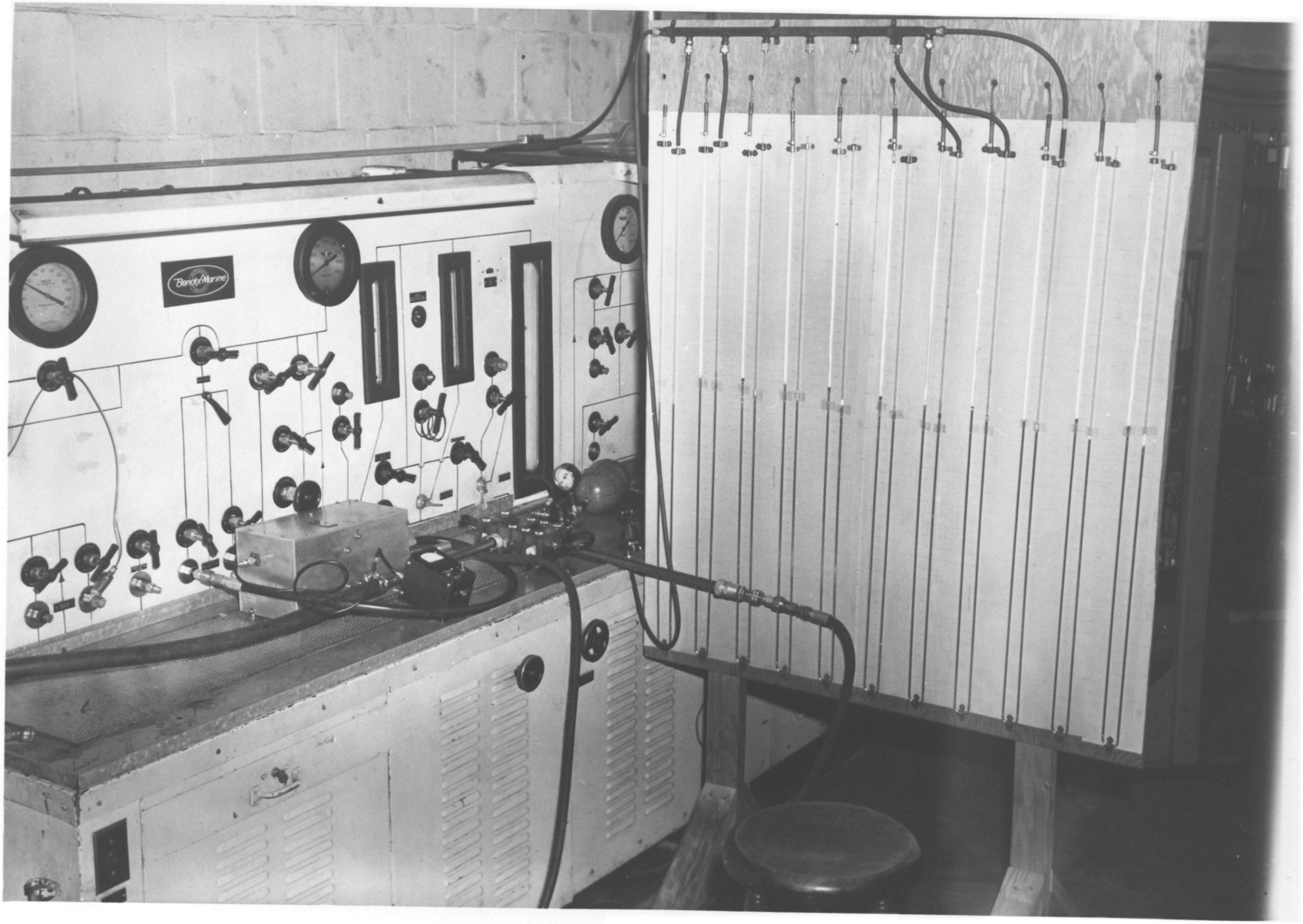
Bendix Marine

Method of taking data

The procedure followed in taking a run of data was as follows:

1. Set a valve opening, tighten clamps
2. Take readings of temperature and pressure at various increasing flows
3. Take readings of temperature and pressure at various decreasing flows
4. Loosen clamps, set a new valve opening and repeat steps 2 and 3.

Results

The main portion of the results are represented in the graphs following this page. These graphs represent the following:

Graph 1 - Pressure drop across the valve and flow at various valve openings.

Graph 2 - Pressure drop along the seat and flow at various valve openings.

Graph 3 - Comparison of pressure drop across the valve for increasing and decreasing flow.

Graph 4 - Flow coefficients.

Graph 5 - Dimensionless pressure-flow curve for converging region.

Graph 6 - Dimensionless pressure-flow curve for the valve.

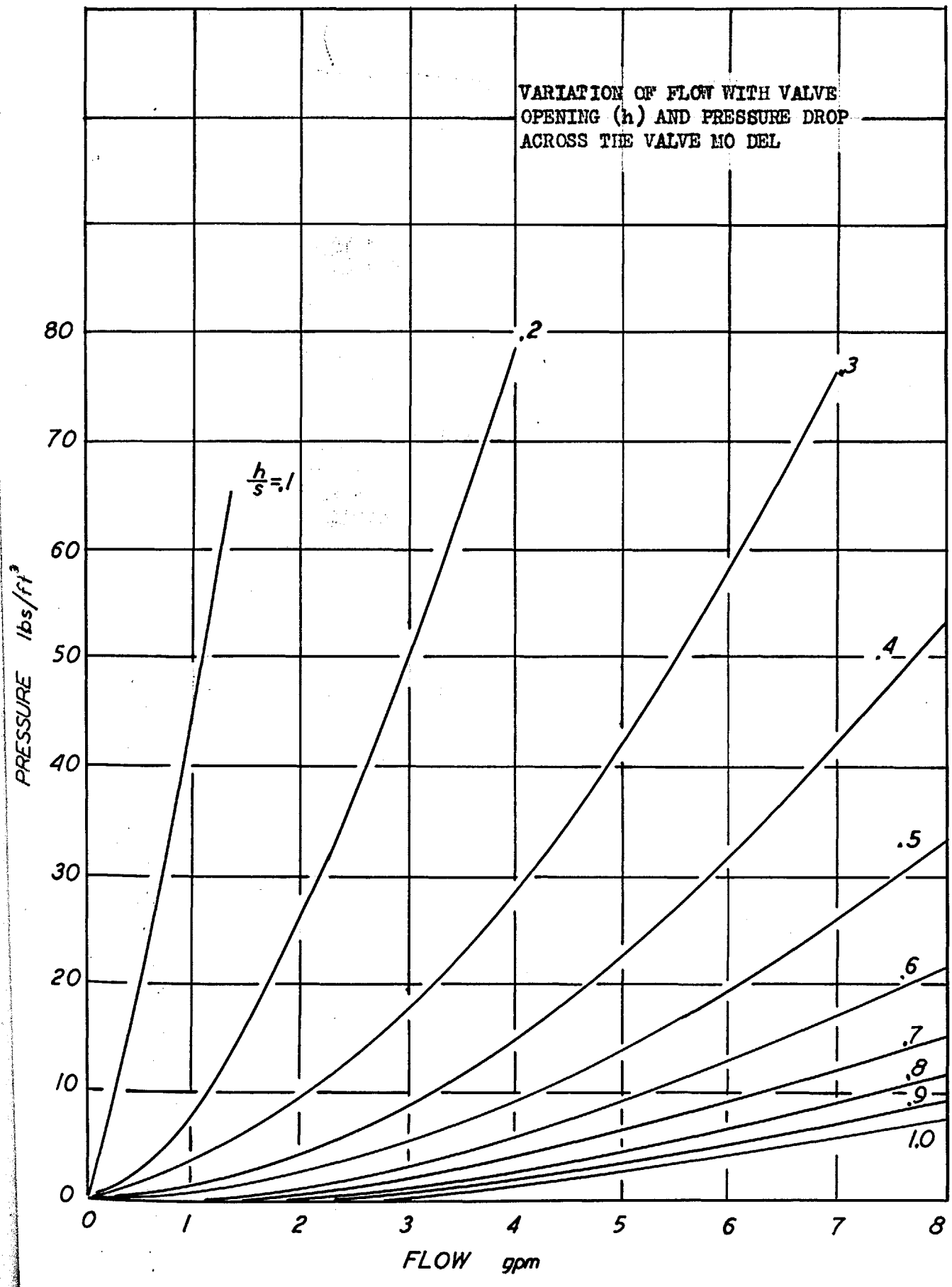
VARIATION OF FLOW WITH VALVE OPENING (h) AND PRESSURE DROP ACROSS THE VALVE MO DEL
PRESSURE lbs/ft²
FLOW gpm
h/s = .1
.2
.3
.4
.5
.6
.7
.8
.9
1.0
0
10
20
30
40
50
60
70
80
0
1
2
3
4
5
6
7
8

GRAPH 1

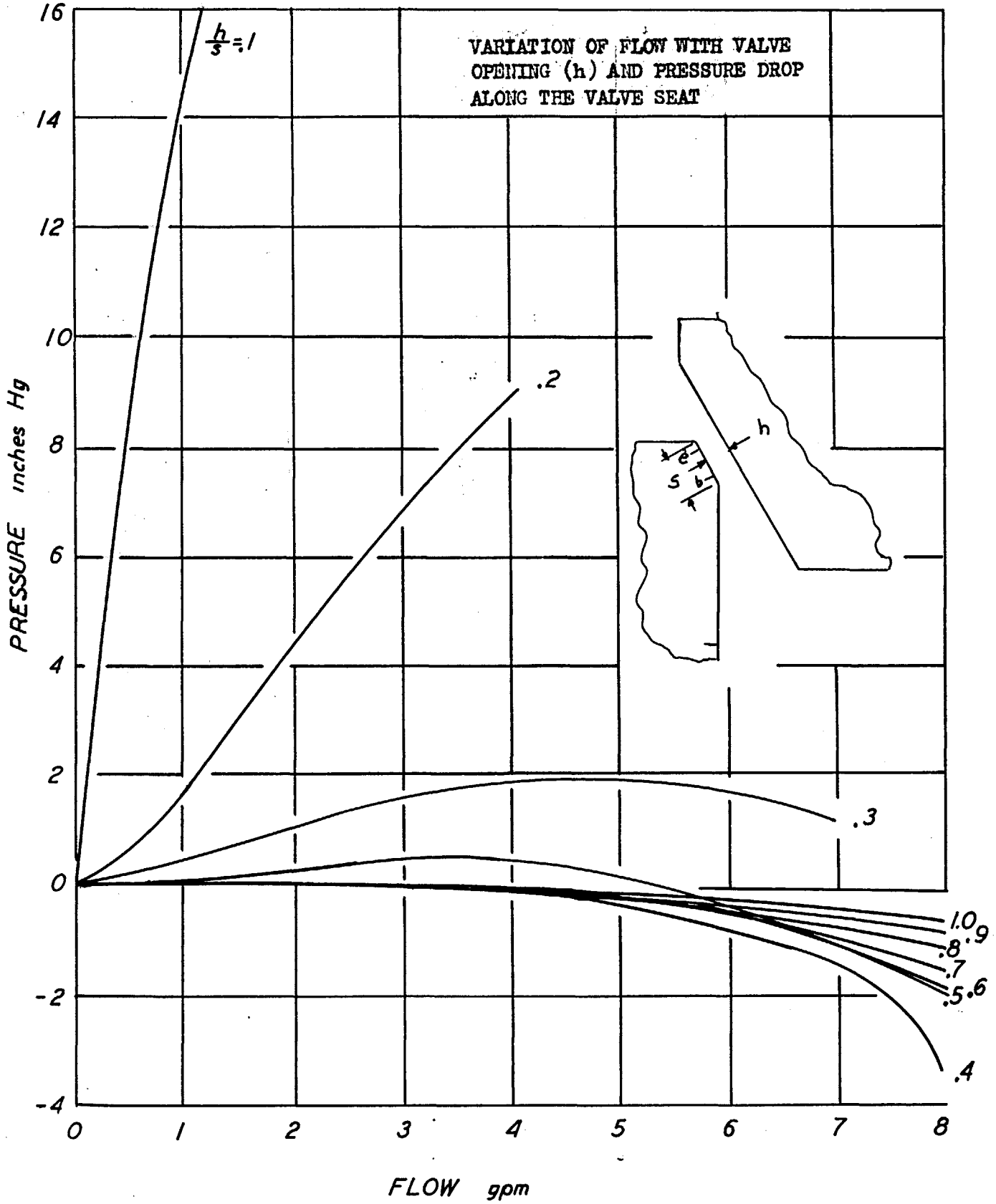
VARIATION OF FLOW WITH VALVE OPENING (h) AND PRESSURE DROP ALONG THE VALVE SEAT
h/s = 1
.2
.3
.4
.5
.6
.7
.8
.9
1.0
h
s
PRESSURE inches Hg
FLOW gpm
16
14
12
10
8
6
4
2
0
-2
-4
0
1
2
3
4
5
6
7
8

GRAPH 2

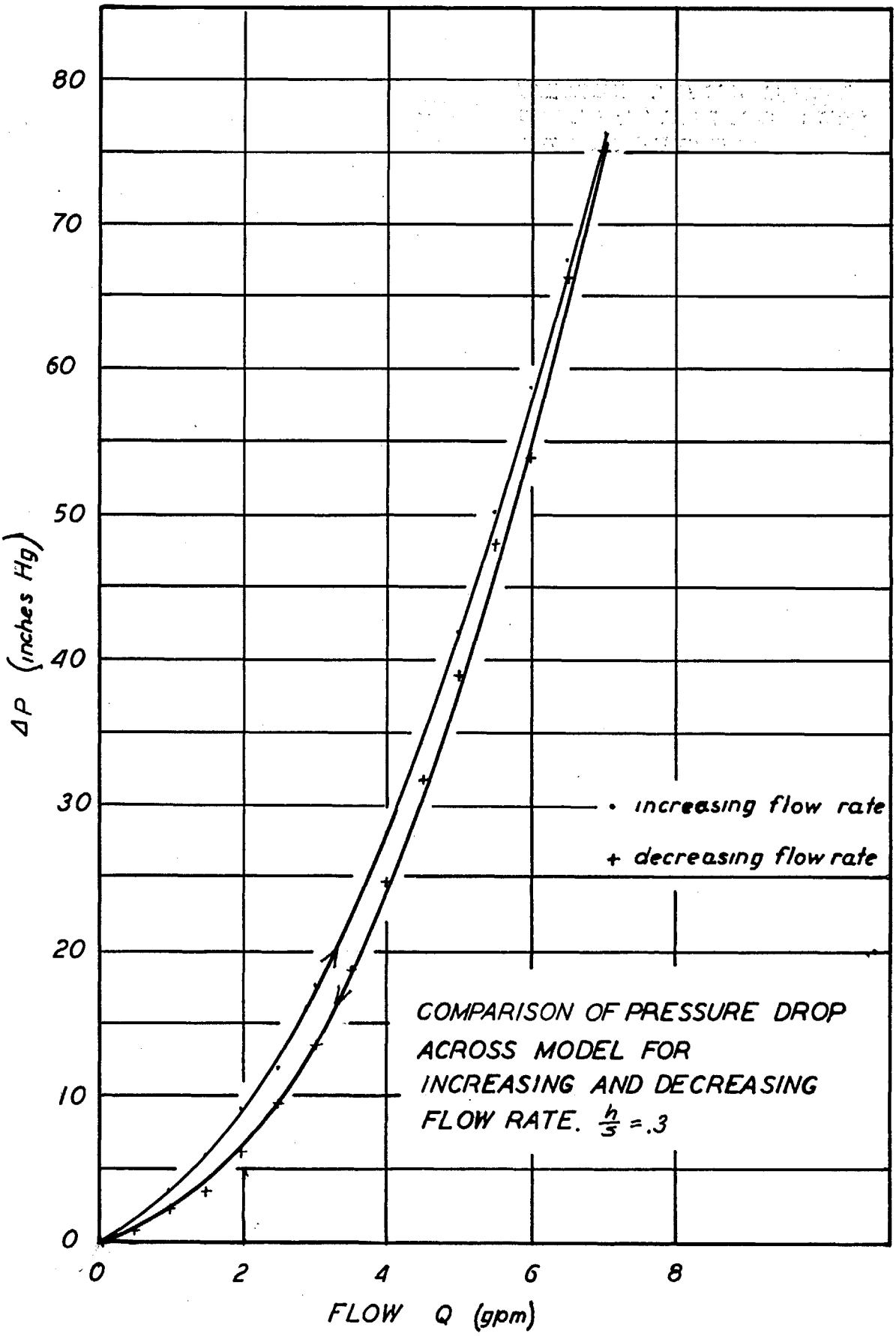
80
70
60
50
40
30
20
10
0
ΔP (inches Hg)
0
2
4
6
8
FLOW Q (gpm)
• increasing flow rate
+ decreasing flow rate
COMPARISON OF PRESSURE DROP ACROSS MODEL FOR INCREASING AND DECREASING FLOW RATE. h/s = .3

GRAPH 3

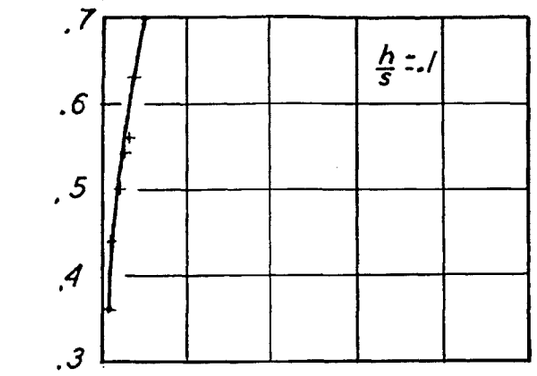

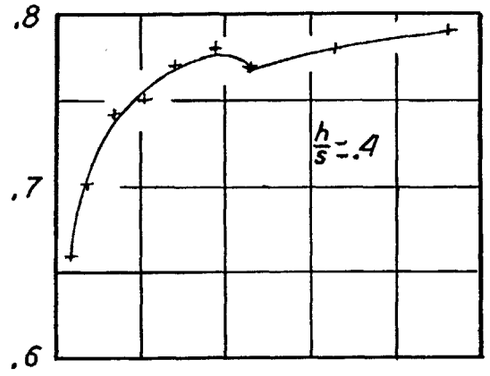

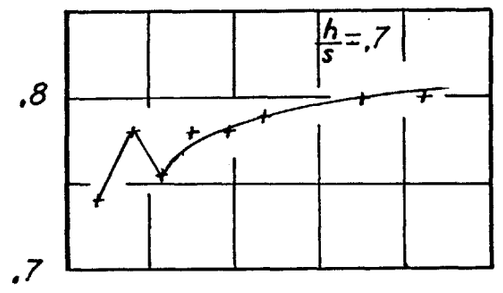

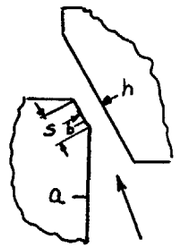

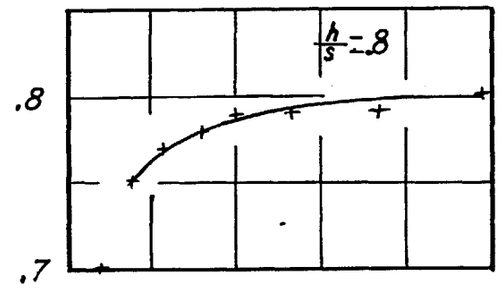

$$C = \frac{Q_{meas.}}{h\sqrt{\frac{2}{3}(P_a - P_b)}}$$

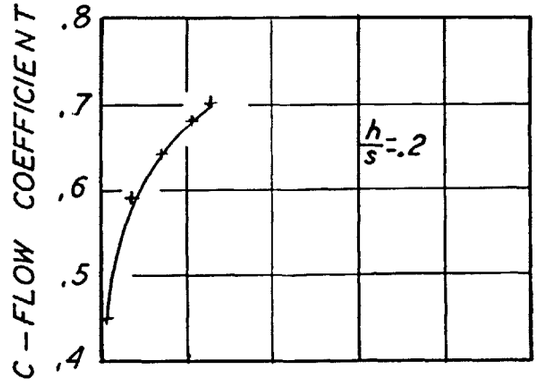

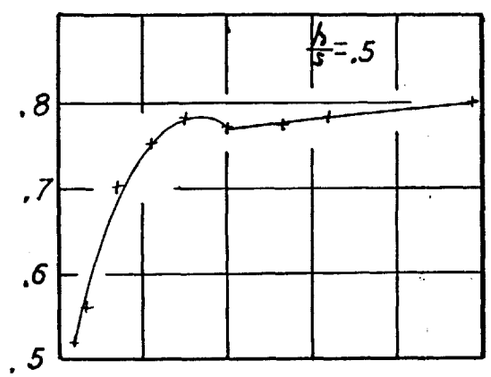

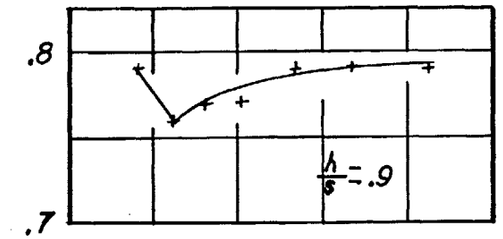

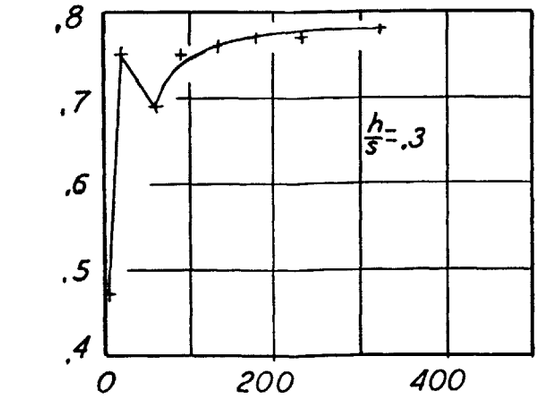

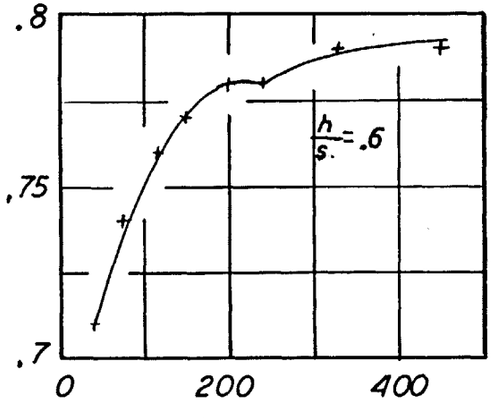

$$Re = \frac{12Q}{\nu}$$

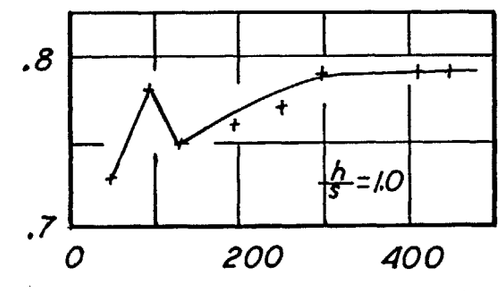

GRAPH 4

FLOW COEFFICIENTS

$\frac{P_a - P_b}{P_a}$

1.2
1.0
.8
.6
.4
.2
0

0 100 200 300 400 500

$Re = \frac{12Q}{\nu}$

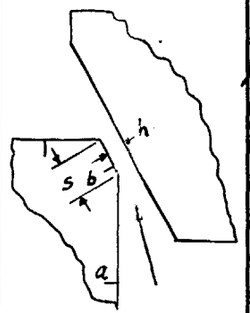

$\frac{h}{s}$

. .1
o .2
x .3
+ .4
□ .5
△ .6
◊ .7
■ .8
▲ .9
◆ 1.0

GRAPH 5

DIMENSIONLESS PRESSURE-FLOW CURVES FOR CONVERGING FLOW REGION

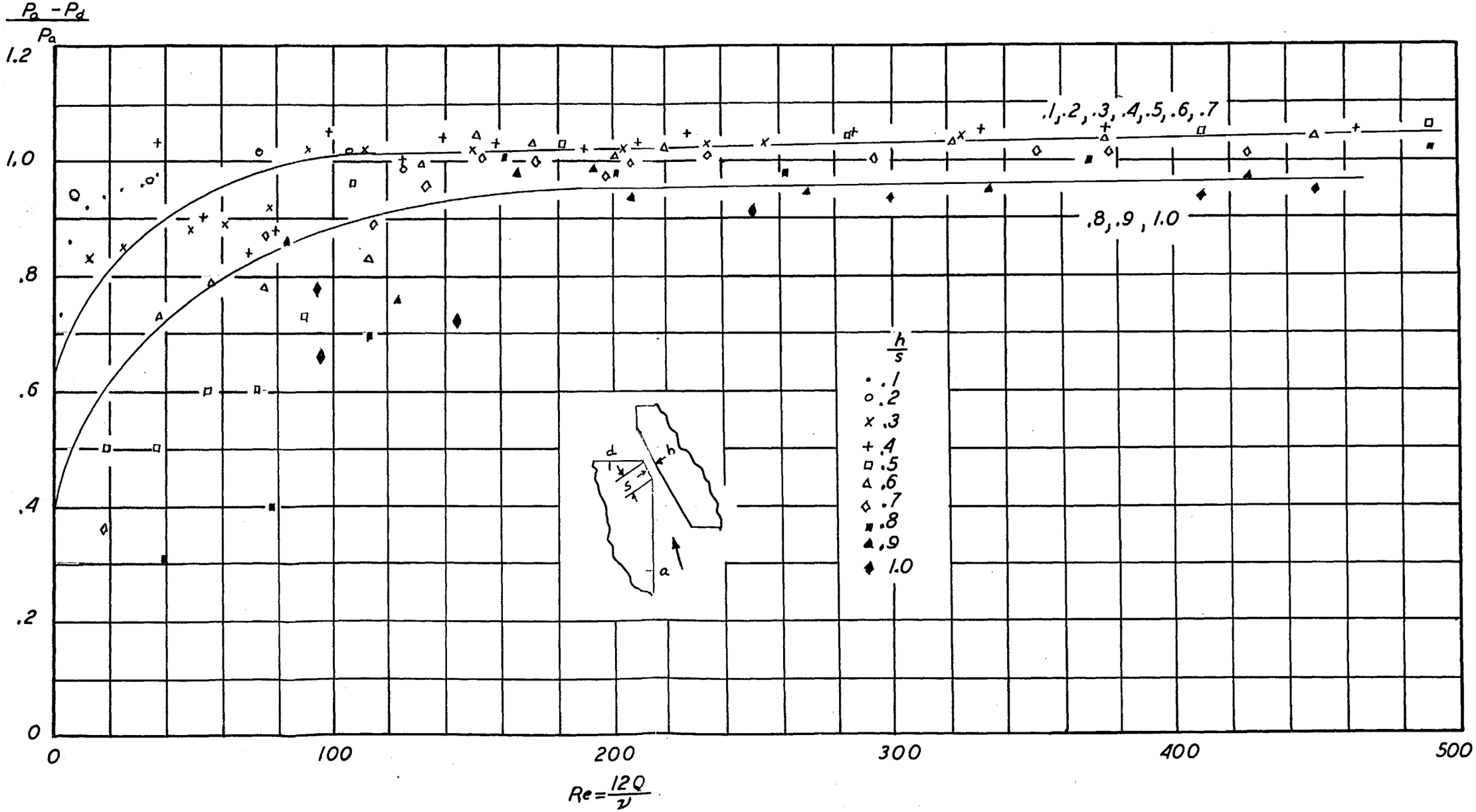

GRAPH 6

DIMENSIONLESS PRESSURE-FLOW CURVE FOR VALVE MODEL

Results and Observations

Interpretation of graphs

It was found necessary to use two curves to represent the points in graph 6 because of the positive discharge pressure (h_d) occuring at opening to seat width ratios greater that .7.

The large spread among the values at low Reynold number for graphs 5 and 6 is due primarily to the difference in discharge pressure at the beginning of the various runs.

It may be noted on graph 6 that at a value of Reynold number of 170 corresponding to a flow of about 4 gpm, the spread between the points is about 3%, a value much lower than any other part of the plot. The discharge pressure at this flow is at a local minimum for values of $^h/_s$ from .4 to 1.0 (i.e. The discharge pressure is greater at flows just higher and lower than 4 gpm)

Graph 5 again contains a single curve to represent rather diverse values. The divergence at higher Reynold numbers is about 10%. A peak may be noted (dotted line) at the same Reynold of 170 referred to for graph 6.

Graph 4 indicates asymptotic value of flow coefficient of .8 for values of $^h/_s$ from .3 to 1.0

The hysteresis observed in graph 3 is within the limits of accuracy of the flowmeter for the method of calibration used. The particular value of $^h/_s$ represented in this plot shows the greatest

divergence over any of the other test runs. It may be assumed, then, that there is no hysteresis in the flow.

The almost constant slope of the curve $h/s = .1$ in graph 1 indicates a laminar flow.

Streamline Observations

In the region just upstream of the seat on the seat side of the valve, a general thickening of the boundary layer was noted. The streamlines bend out into the stream and line themselves up with the seat to decrease the amount of bending required at the entrance to the seat region. (Fig. 4) The ability of the streamlines on the seat side to line themselves up with the seat decreases with increasing flow rate, but increases with larger openings.

At only very low flow rates - up to 0.5 gpm - and relatively large valve openings - $h/s = .8$, .9, 1.0 - was it possible to observe a continuous streamline in the region downstream of the seat. At all other combinations of valve opening and flow rate, a high degree of dispersion of the air bubbles was noted as the stream left the seat region. The initially solid line of air bubbles was reduced to a multitude of very small air bubbles in the downstream region. These observations imply a high degree of turbulence occuring in the seat region.

The pattern of the air bubbles downstream

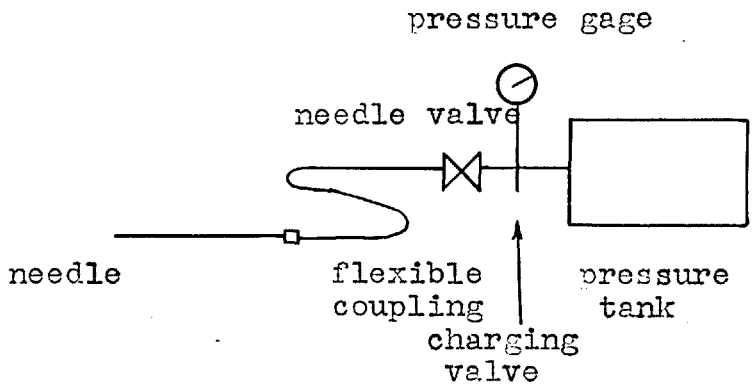

Schematic of air injector

Figure 3

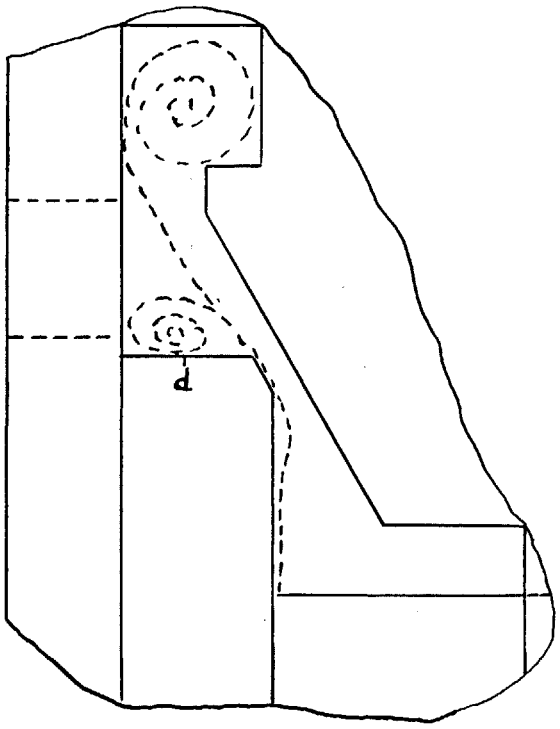

Boundary layer and vortex pattern

Figure 4

of the seat indicated a vortex at point d. (See fig. 4). The degree of vorticity seemed to be the greatest at a value of $^{h}/_{s}$ of .3 and a flow of 7 gpm . Under these conditions, a solid column of air somewhat resembling a whirlpool was observed.

A counter-rotating vortex was observed against the poppet shaft. This vortex encompassed a larger area than the other, but seemed to be much less violent.

General Observations

1). For values of $^{h}/_{s}$ up to .3 and flow rates less than 3 gpm , the pressure drop across the seat is very nearly evenly distributed along the seat width.

2). For values of $^{h}/_{s}$ from .4 to 1.0 and flow rates up to 3 gpm, the pressure drop across the seat occurs along the downstream half of the seat.

3). For values of $^{h}/_{s}$ from .3 to 1.0 and flow rates above 4 gpm, there occurs a general decrease in pressure at the upstream end of the seat as the flow is increased, accompanied by a continuous increase in pressure at the center of the seat, resulting in a pressure rise in the direction of flow along the upstream half of the valve.

4). The pressure on the upstream face of the poppet is almost constant along the face, decreasing by only about 10% up to the entrance of the seat. The pressure near the upstream end of the poppet

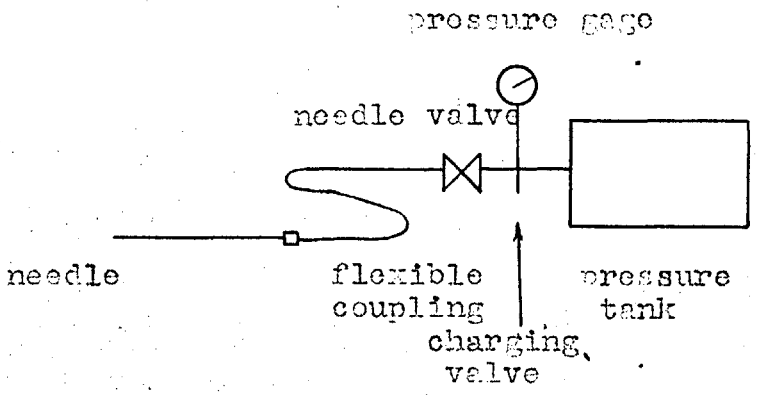

Schematic of air injector

Figure 3

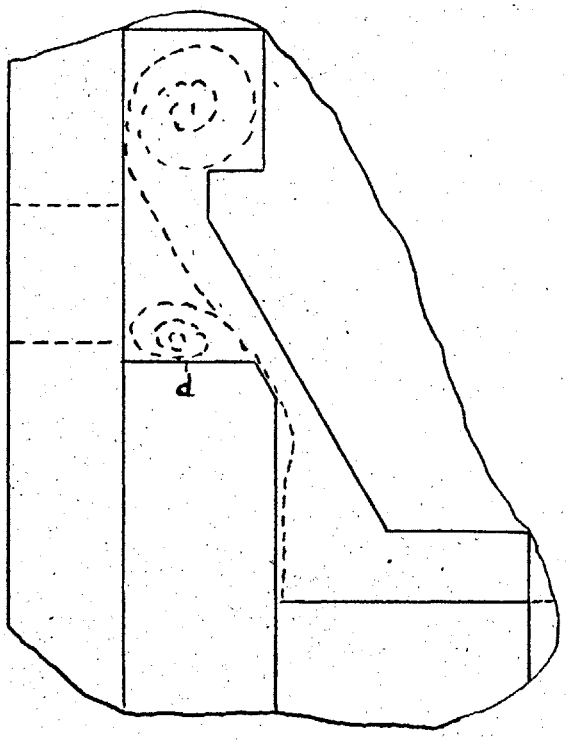

Boundary layer and vortex pattern

Figure 4

face agrees within 1% in most cases, with inlet pressure.

5). The pressure on the downstream face of the poppet is always somewhat higher than the exhaust pressure. The difference between the pressure on the poppet face downstream of the seat and the exhaust pressure increases with increasing flow due to the accelerated vorticity in the exhaust region at higher flow rates.

6). There is a high degree of sensitivity to exhaust pressure in the values of pressures on the valve seat, and in the downstream region. Minute changes in exhaust pressure are mirrored in all the pressures past the entrance to the valve seat.

7). Air streamers trailing from the downstream end of the seat were noticed at almost all values of $^{h}/_{s}$ and higher flow rates, indicating the possibility of cavitation at the valve seat.

Conclusions and Recommendations

The flow in a valve cannot be adequately described without further investigation. The flow in the seat region must be studied with an even larger scale model than was used for this investigation. The model should be so designed that the motion of the poppet relative to the seat to obtain larger openings takes place along a direction perpendicular to the seat face. With corresponding pressure taps located on the poppet and the seat, there will be no change in the relative position of the pressure taps as the valve opening is increased and a complete study of the pressures on both sides of the channel may be conducted.

The only limitation to the size of the model to be used is the maximum flow which may be obtained from the oil pump.

Further investigation should be carried out on the affect of different seat widths, different poppet angles, various poppet geometries and various exhaust pressures on the pressures and flow in the valve.

For the purpose of establishing characteristic values of pressure and flow, any further investigation should be conducted with fewer variables. In the case of graph 5, for example, a better representation of the flow in the converging region would have been obtained if the pressure Pb could have been maintained constant. In like manner, for graph 6, the exhaust pressure pd should be kept constant.

In order to best photograph the streamline pattern, a system of side lighting through the bottom plate of glass of the model should be used. The upper glass plate should be completely isolated from ambient light. No reflecting surface should be placed under the model as it has a tendency to cause an uneven distribution of light resulting in glared spots on the photograph. The side lighting utilizes the refraction of light at the air-oil boundary to highlight the air stream.

APPENDIX I

EXPERIMENTAL DATA

h_a	h_b	h_d	h_e	Q	T	h/s
3.7	2.9	1.0	1.7	.1	62	.1
8.5	6.0	1.2	3.0	.2	62	
17.3	11.1	1.4	5.2	.4	62	
27.2	16.0	1.6	7.3	.6	62	
38.3	20.8	1.7	9.2	.8	62	
51.1	25.6	1.8	11.2	1.0	62	
71.5	32.5	1.8	13.5	1.2	62	
.9	.6	.1	.3	.2	66	.2
7.2	2.7	.2	1.2	1.0	66	
15.9	4.1	- .4	1.3	2.0	67	
38.6	7.9	- .7	2.4	3.0	67	
72.4	15.1	1.0	6.2	4.0	63	
.2	.1	- .2	- .1	.2	64	.3
2.8	1.3	.5	.8	1.0	62	
10.5	3.1	1.2	2.0	2.0	62	
13.1	3.3	1.1	2.1	2.5	62	
17.4	2.4	- .3	1.0	3.0	62	
22.2	2.8	- .4	1.2	3.5	64	
27.6	3.0	- .6	1.1	4.0	65	
33.7	3.1	- .8	1.3	4.5	67	
40.9	3.4	- .9	1.6	5.0	68	
49.1	3.6	-1.1	1.8	5.5	69	
51.1	3.6	-1.7	1.8	6.0	71	
65.5	3.4	-2.3	1.7	6.5	71	
73.5	2.9	-2.8	1.7	7.0	77	

h_a	h_b	h_d	h_e	Q	T	h/s
.1	- .2	- .4	- .3	.5	69	.4
1.2	.2	- .1	.2	1.0	67	
3.1	.8	.3	.6	1.5	67	
5.0	1.3	.8	1.1	2.0	67	
7.5	1.8	.9	1.4	2.5	67	
9.1	1.0	.1	.6	3.0	67	
12.0	1.1	- .1	.6	3.5	67	
13.9	.4	- .7	.1	4.0	67	
17.3	.6	- .5	.4	4.5	67	
21.3	.6	- .5	.5	5.0	70	
26.2	.5	- .9	.6	5.5	70	
30.4	.1	-1.4	.4	6.0	70	
35.0	- .2	-1.8	.5	6.5	75	
40.2	- .7	-2.1	.4	7.0	78	
44.2	-1.1	-2.4	.4	7.5	80	
49.7	-1.7	-2.6	.4	8.0	85	
.7	.4	.4	.2	.5	70	.5
1.6	.8	.8	.9	1.0	68	
2.7	1.3	1.1	1.3	1.5	68	
4.4	1.8	1.7	1.8	2.0	68	
5.3	1.7	1.4	1.6	2.5	68	
6.0	.9	.5	.9	3.0	68	
6.8	.0	- .3	0	3.5	68	
8.4	- .1	- .4	0	4.0	70	
10.5	- .1	- .3	.1	4.5	72	
13.4	- .1	- .3	.2	5.0	72	
15.9	- .3	- .4	.3	5.5	75	
18.6	- .5	- .8	.3	6.0	75	
21.5	- .8	-1.0	.4	6.5	75	
24.8	-1.2	-1.2	.4	7.0	78	
27.3	-1.7	-1.3	.3	7.5	83	
28.9	-3.1	-1.7	.2	8.0	87	
33.8	-4.6	-1.5	.1		88	

h_a	h_b	h_d	h_e	Q	T	$h/_s$
0	.1	-.2	-.2	.5	70	.6
.6	.2	.2	.1	1.0	70	
1.4	.5	.3	.4	1.5	70	
2.3	.6	.5	.6	2.0	70	
3.7	.9	.7	.9	2.5	70	
4.3	.8	.7	.8	3.0	70	
4.8	.1	.0	.2	3.5	70	
5.7	.3	-.3	.1	4.0	70	
7.2	.3	-.2	.1	4.5	70	
9.0	.2	-.1	.2	5.0	72	
10.5	.4	-.2	.2	5.5	72	
12.5	.6	-.4	.2	6.0	75	
14.8	.7	-.5	.3	6.5	75	
16.6	.9	-.6	.3	7.0	78	
18.6	1.3	-.7	.2	7.5	80	
20.9	1.8	-.8	.2	8.0	83	
-.2	-.5	-.5	-.5	1	70	.7
.5	-.2	-.2	-.2	1.5	70	
1.3	.2	.2	.2	2.0	70	
2.3	.5	.5	.6	2.5	70	
2.8	.3	.3	.4	3.0	70	
3.5	.1	.1	.2	3.5	70	
4.1	-.1	.0	.1	4.0	70	
5.2	-.1	.0	.1	4.5	70	
6.6	-.1	.2	.2	5.0	72	
7.6	-.4	.0	.2	5.5	72	
8.9	-.5	-.1	.2	6.0	72	
10.6	-.6	-.1	.3	6.5	76	
11.9	-.8	-.2	.3	7.0	80	
13.5	-1.1	-.2	.2	7.5	80	
15.2	-1.4	-.3	.2	8.0	82	

h_a	h_b	h_d	h_e	Q	T	h/s
1.3	1.0	.9	1.1	1	71	.8
2.9	2.5	1.8	2.0	2	71	
2.7	.8	.8	.9	3	71	
3.2	- .1	0	.1	4	72	
4.9	- .1	.1	.2	5	72	
6.9	- .4	.2	.2	6	75	
9.2	- .6	0	.3	7	82	
11.4	-1.2	-.2	.1	8	87	
.5	- .6	-.1	-.6	1	73	.9
.8	.2	.1	.1	2	73	
1.9	.4	.5	.4	3	73	
2.5	- .1	.1	.1	4	73	
4.0	- .1	.3	.3	5	73	
5.7	0	.3	.5	6	76	
7.5	- .1	.4	.6	7	79	
9.5	- .5	.3	.6	8	82	
-.3	- .4					1.0
.8	.3					
1.7	.4					
2.0						
3.3						
4.6						
6.2						
7.9						

APPENDIX II

CALCULATIONS - FLOW COEFFICIENTS AND DIMENTIONLESS PRESSURES

$$C = \frac{Qc}{A_2\sqrt{\frac{2}{\rho}(Pa-Pb)}}$$ As defined in the Preliminary Analysis.

$(Pa-Pb) = \frac{\rho(Hg)xg}{12}(ha-hb)$

Q_c = oil flow - ft^3/sec

ρ (Hg) = 26.30 $Slugs/ft^3$

g = 32.2 ft/sec^2

$A_2 = \frac{h}{144}$

Values of density for oil (ρ) as a function of temperature are given in Appendix III. It may be noted that in the range from 60^0 F to 90^o F, the density change is less than 2%. For the calculation of flow coefficients, the density was considered invariant with temperature at 1.65 $slugs/ft^3$.

The Reynolds number with respect to valve Re_h opening is defined as

$$Re_h = \frac{VD}{\nu} = \frac{Q_c\, h/12}{h/144 \times \nu} = \frac{12\,Q_c}{\nu}$$

V= Velocity of flow at valve seat (ft/sec)

D= Characteristic length (ft)

ν = Kinematic viscosity (ft^2/sec)

h= Valve opening (inches)

The variation of kinematic viscosity (ν) with temperature is represented in a graph in Appendix III.

$h/_s$= ratio of valve opening to seat width

Q= oil flow through valve (gallons/min.)

$\frac{Pa-Pb}{Pa}$ = Dimensionless pressure drop in converging region

$\frac{Pa-Pd}{Pa}$ = Dimensionless pressure drop across the valve

Pb-Pe = Pressure drop along the valve seat

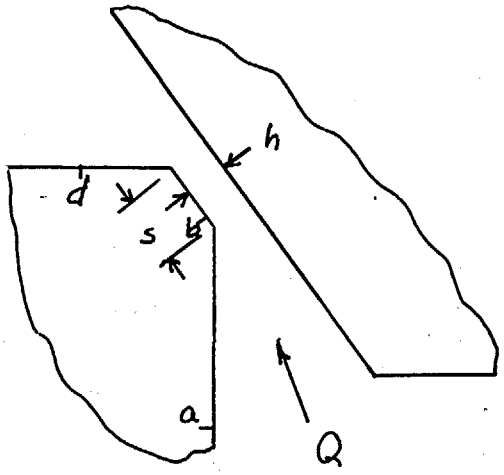

$h/_s$	Q	$\frac{Pa-Pb}{Pa}$	$\frac{Pa-Pd}{Pa}$	Pb-Pe	C	$Re_{(h)}$
.1	.1	.23	.73	1.2		3.0
	.2	.29	.86	3.0	.37	6.1
	.4	.36	.92	6.0	.44	12.2
	.6	.41	.94	8.8	.50	18.4
	.8	.46	.96	11.6	.54	24.5
	1.0	.50	.96	14.0	.56	31.0
	1.2	.55	.98	17.0	.63	37.0
.2	.2	.41	.94	.3	.45	6.8
	1.0	.63	.97	1.7	.59	34.
	2.0	.74	1.02	4.4	.64	72
	3.0	.80	1.02	6.7	.68	107
	4.0	.79	.99	8.9	.70	126
.3	.2	.70	2.6	.1	.47	6.7
	1.0	.57	.85	.5	.75	25
	2.0	.70	.89	1.0	.69	61
	2.5	.75	.92	1.2	—	77
	3.0	.86	1.02	1.4	.75	92
	3.5	.87	1.02	1.6	—	112
	4.0	.90	1.02	1.9	.76	133
	4.5	.91	1.02	1.9	—	150
	5.0	.90	1.02	1.7	.77	180

$h/_s$	Q	$\frac{Pa-Pb}{Pa}$	$\frac{Pa-Pd}{Pa}$	Pb-Pe	C	Re(h)
.3	5.5	.93	1.02	1.7	—	204
	6.0	.94	1.03	1.7	.77	235
	6.5	.95	1.03	1.6	—	255
	7.0	.96	1.04	1.1	.78	325
.4	.5	2.64	4.5	.1	.66	18.5
	1.0	.83	1.03	.1	.70	37
	1.5	.74	.90	.2	—	53
	2.0	.74	.84	.3	.74	70
	2.5	.76	.88	.4	—	80
	3.0	.89	.99	.4	.75	105
	3.5	.91	1.00	.4	—	123
	4.0	.97	1.04	.3	.77	140
	4.5	.97	1.03	.1	—	158
	5.0	.98	1.02	0.0	.78	190
	5.5	.99	1.03	-.1	—	210
	6.0	1.00	1.05	-.4	.77	228
	6.5	1.01	1.05	-.7	—	287
	7.0	1.02	1.05	-1.1	.78	332
	7.5	1.02	1.05	-1.5	—	375
	8.0	1.03	1.05	-2.1	.79	465
.5	.5	.43	.50	.2	.52	19
	1.0	.47	.50	-.1	.56	36
	1.5	.51	.60	.1	—	54
	2.0	.59	.60	.2	.70	72
	2.5	.68	.73	.1	—	90
	3.0	.85	.93	.1	.75	108
	3.5	1.00	1.04	0.0	—	126
	4.0	1.01	1.04	-.1	.78	152
	4.5	1.02	1.03	-.3	—	181
	5.0	1.01	1.02	-.3	.77	201
	5.5	1.02	1.03	-.7	—	242
	6.0	1.03	1.04	-.9	.77	264
	6.5	1.04	1.04	-1.2	—	285
	7.0	1.05	1.05	-1.5	.78	322
	7.5	1.06	1.05	-2.0	—	410
	8.0	1.11	1.06	-3.4	.80	490

$h/_s$	Q	$\frac{Pa-Pb}{Pa}$	$\frac{Pa-Pd}{Pa}$	Pb-Pe	C	$Re_{(h)}$
.6	.5	43.5	38.0	.2	—	19
	1.0	.74	.73	0.0	.71	38
	1.5	.68	.78	.1	—	57
	2.0	.72	.78	0.0	.74	76
	2.5	.74	.78	-0.0	—	91
	3.0	.82	.83	-0.0	.76	114
	3.5	.99	1.0	-.1	—	133
	4.0	1.05	1.05	-.3	.77	152
	4.5	1.04	1.03	-.3	—	171
	5.0	1.02	1.01	-.4	.78	201
	5.5	1.04	1.02	-.6	—	221
	6.0	1.05	1.03	-.8	.78	242
	6.5	1.04	1.03	-1.0	—	286
	7.0	1.05	1.03	-1.3	.79	332
	7.5	1.07	1.04	-1.6	—	375
	8.0	1.09	1.04	-2.0	.79	450
.7	1.0	-1.36	-1.36	0.0	.74	38
	1.5	1.51	1.51	-.1	—	57
	2.0	.91	.87	0.0	.78	76
	2.5	.81	.79	-.1	—	95
	3.0	.89	.89	-.1	.76	114
	3.5	.98	.96	-.1	—	133
	4.0	1.02	1.01	-.1	.78	152
	4.5	1.01	1.0	-.2	—	171
	5.0	1.02	.97	-.4	.78	196
	5.5	1.05	1.0	-.6	—	216
	6.0	1.06	1.01	-.7	.79	235
	6.5	1.06	1.0	-.9	—	293
	7.0	1.07	1.02	-1.1	.80	350
	7.5	1.08	1.02	-1.3	—	375
	8.0	1.09	1.02	-1.6	.80	425
.8	1.0	.20	.31	-.0	.70	39
	2.0	.35	.40	.5	.70	79
	3.0	.70	.69	-.1	.77	113
	4.0	1.03	1.01	-.1	.78	161
	5.0	1.01	.98	-.3	.79	201
	6.0	1.05	.98	-.6	.79	263
	7.0	1.07	1.00	-.9	.79	370
	8.0	1.10	1.02	-1.3	.80	490
.9	1.0	2.13	1.20	-0.0	.29	42
	2.0	.80	.86	0.0	.79	83
	3.0	.82	.76	-.1	.76	124
	4.0	1.05	.98	-.2	.77	166
	5.0	1.03	.94	-.5	.77	207
	6.0	.99	.95	-.5	.79	270
	7.0	.98	.95	-.7	.79	334
	8.0	1.05	.97	-1.1	.79	425

$h/_s$	Q	$\frac{Pa-Pb}{Pa}$	$\frac{Pa-Pd}{Pa}$	Pb-Pe	C	$Re_{(h)}$
1.0	1.0	-.56	-.37	-.1	.73	50
	2.0	.67	.67	-.0	.78	96
	3.0	.76	.73	-.1	.75	145
	4.0	.99	.99	-.0	.80	193
	5.0	.99	.92	-.3	.77	250
	6.0	.99	.94	-.4	.79	300
	7.0	1.02	.94	-.6	.79	410
	8.0	1.04	.95	-.8	.79	450

APPENDIX III

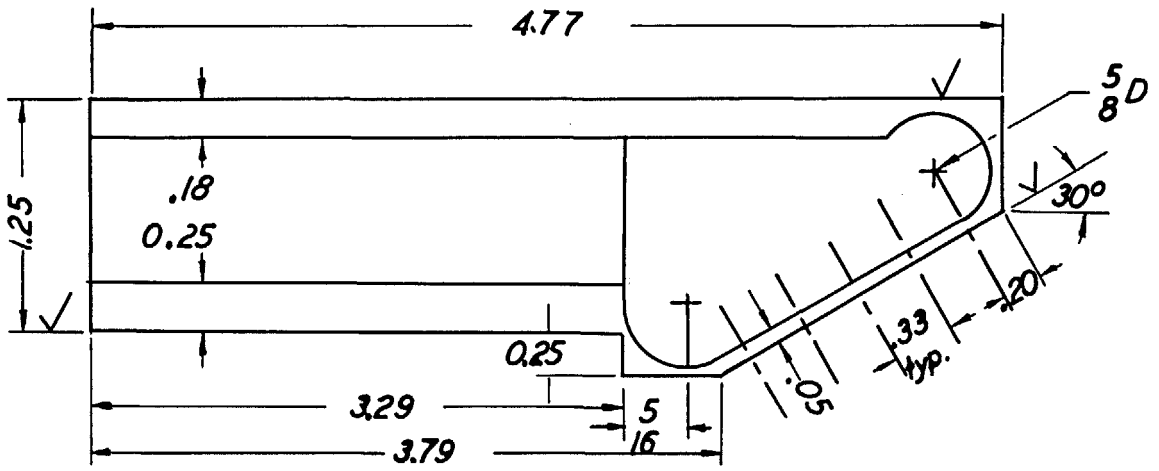

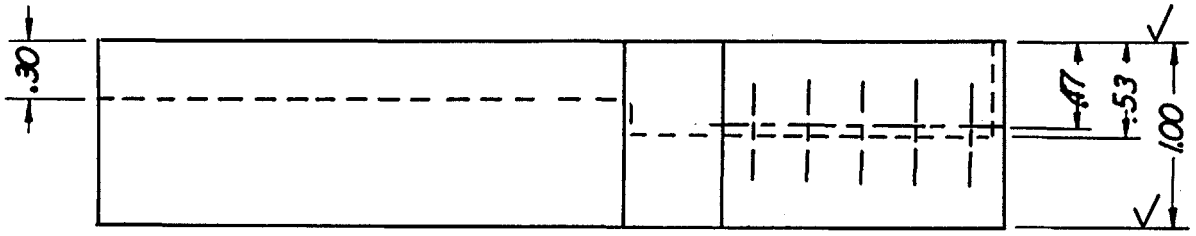

STEEL	POPPET	
FULL SCALE		
MAKE 1		
9-24-53		

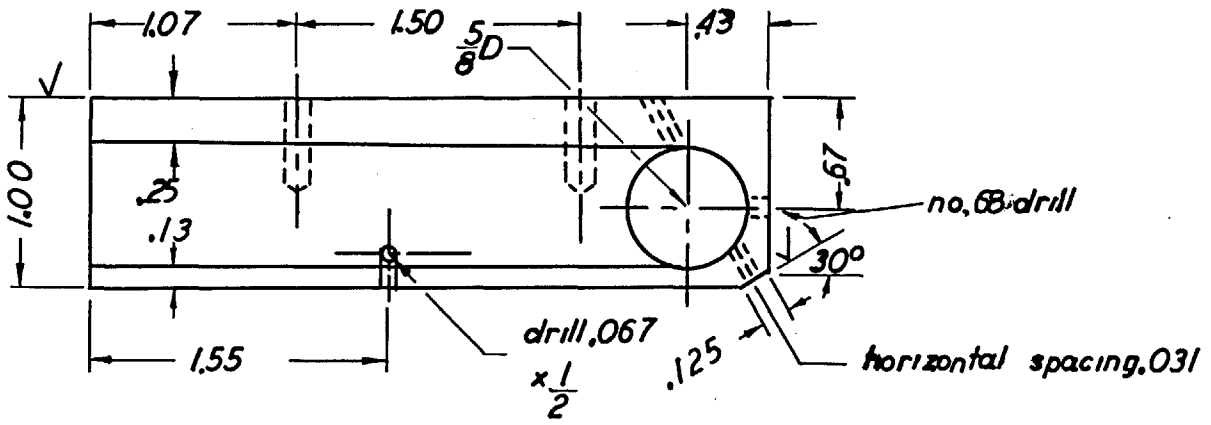

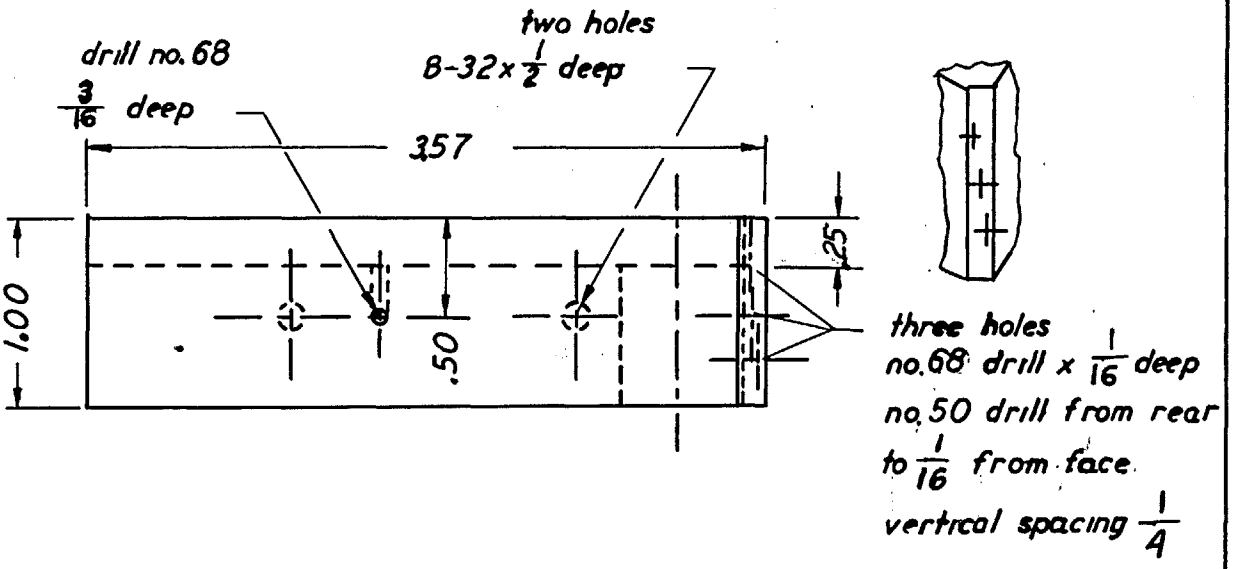

STEEL	SEAT	2
FULL SCALE		
MAKE 1		
9-24-53		

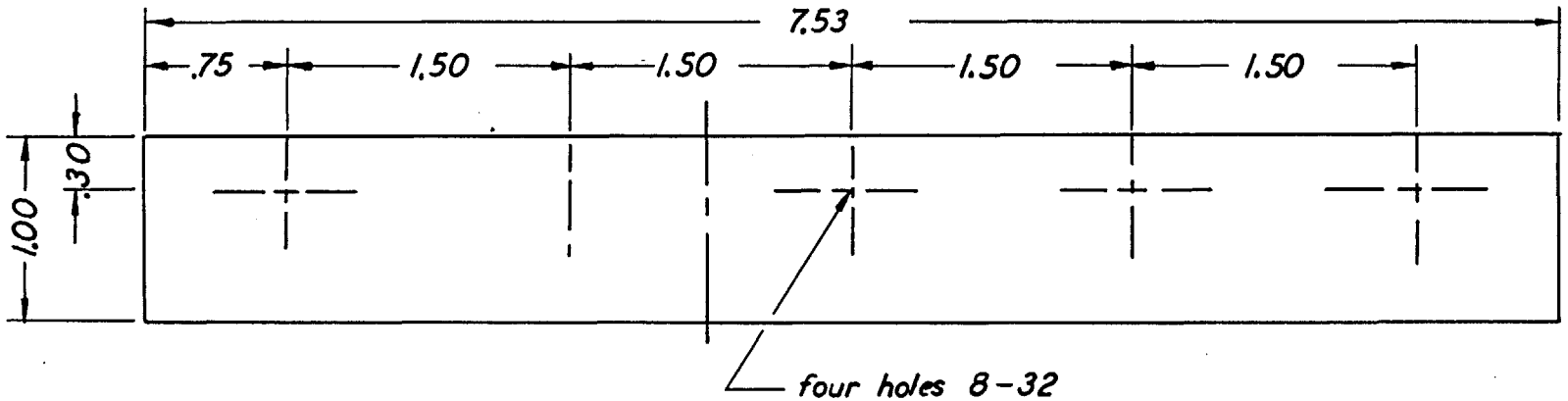

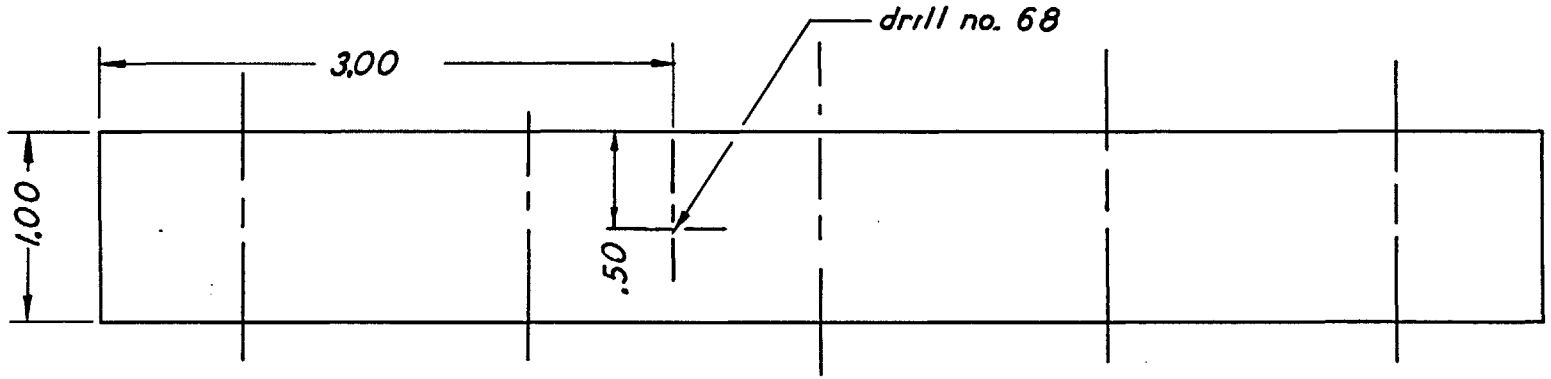

STEEL	FRAME 1	3
FULL SCALE		
MAKE 1		
9-24-53		

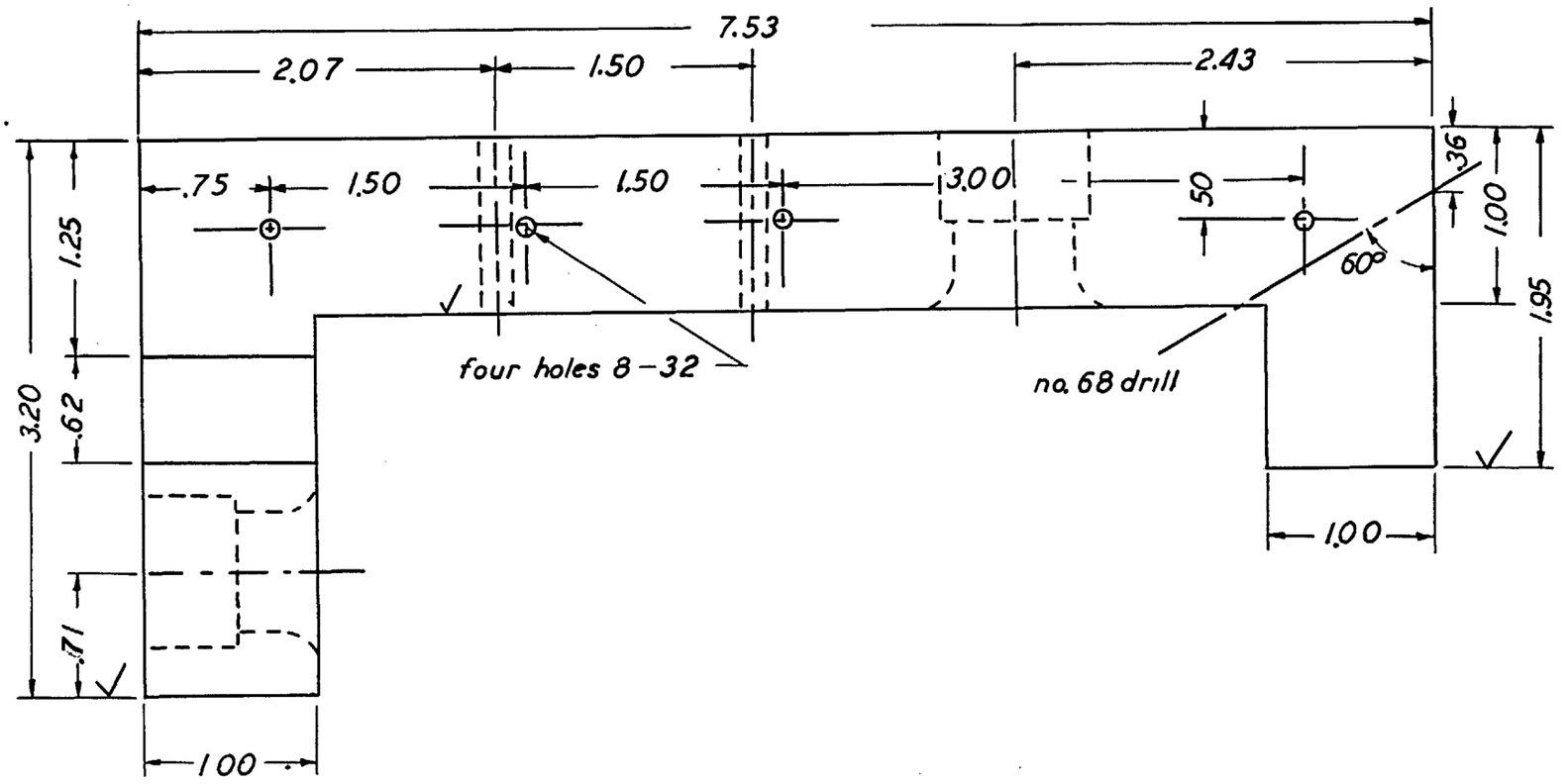

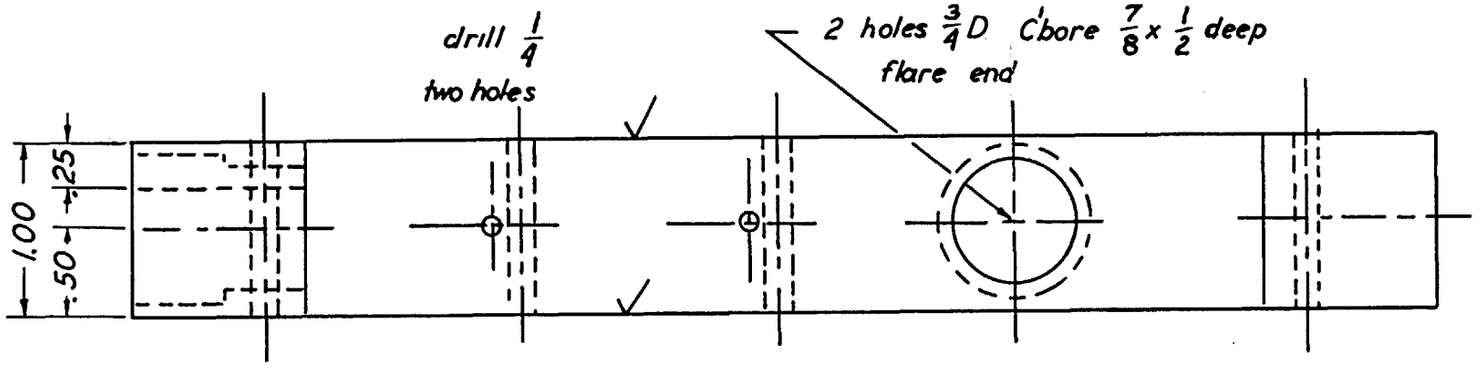

STEEL	FRAME 2	4
FULL SCALE		
MAKE 1		
9-24-53		

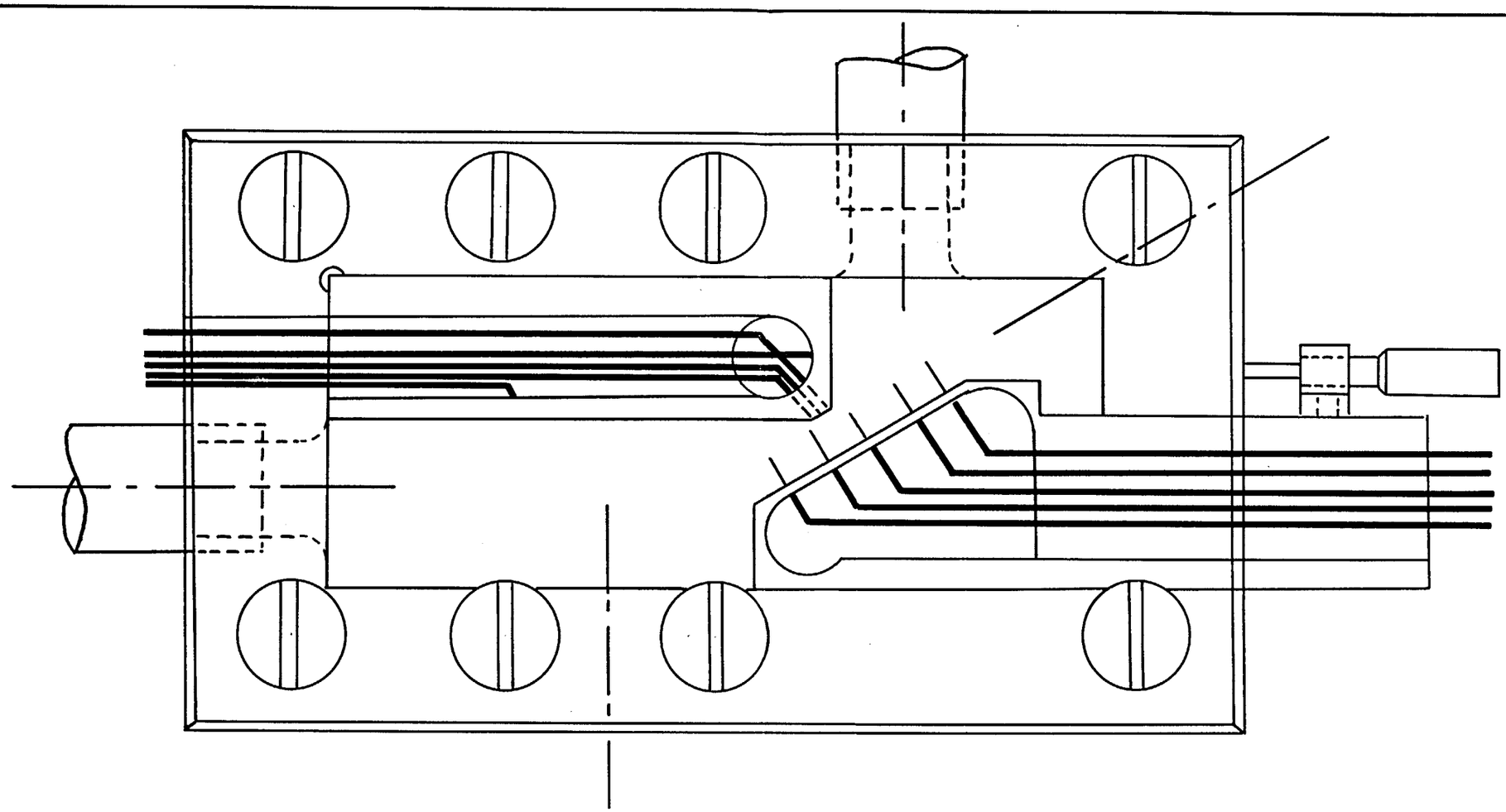

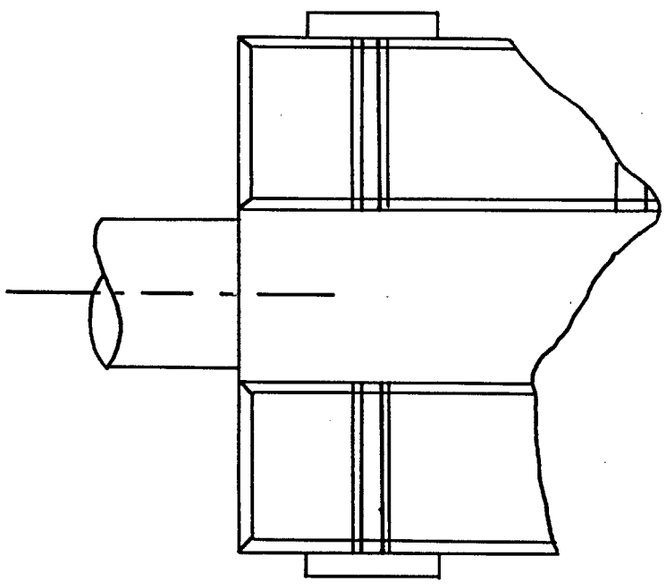

STEEL	ASSEMBLY	5
FULL SCALE		
MAKE 1		
9-24-53		

APPENDIX IV

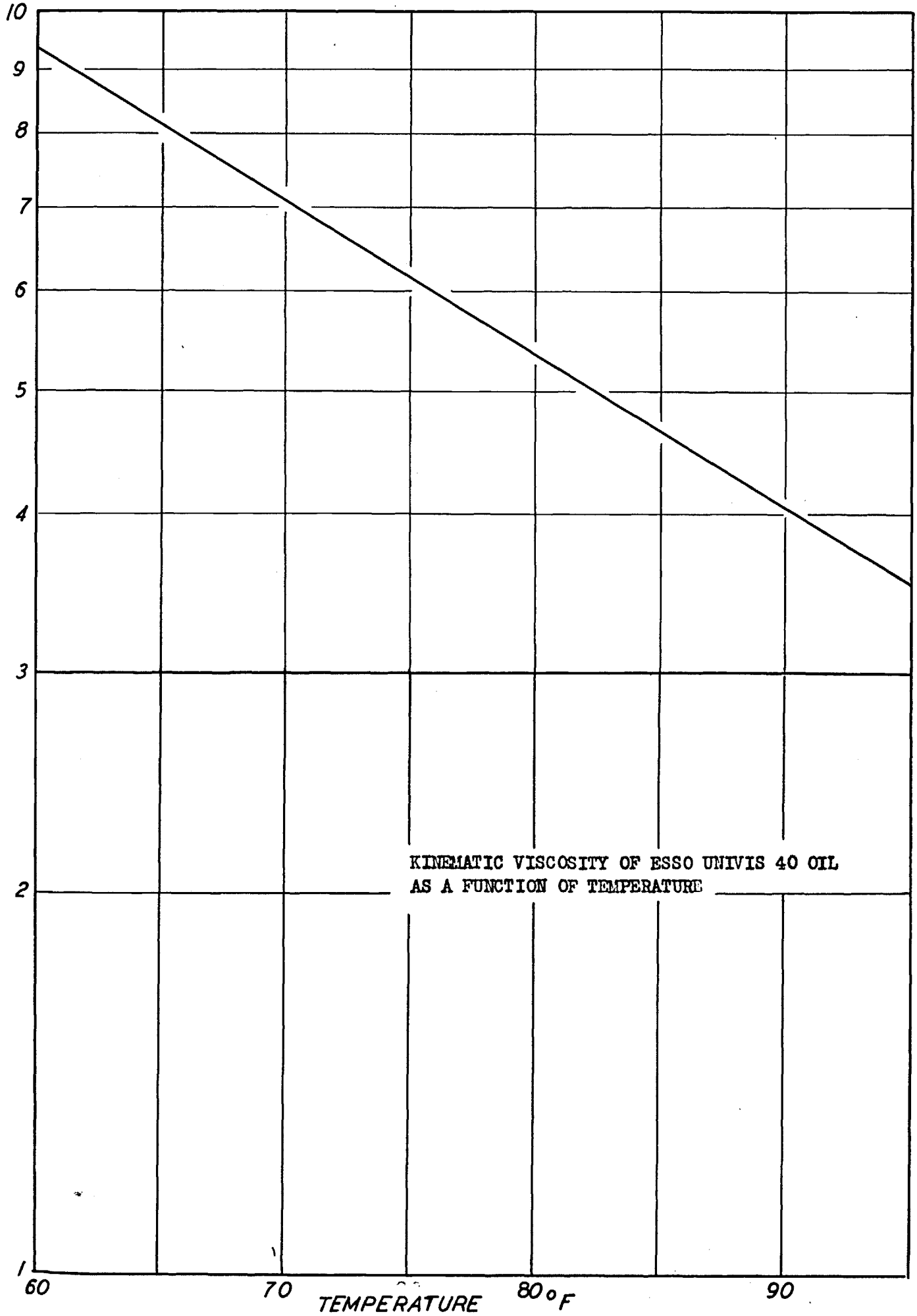
10
9
8
7
6
5
4
3
2
1
60
70
80°F
90
TEMPERATURE
ν x 10⁻⁴ ft²/sec
KINEMATIC VISCOSITY OF ESSO UNIVIS 40 OIL
AS A FUNCTION OF TEMPERATURE

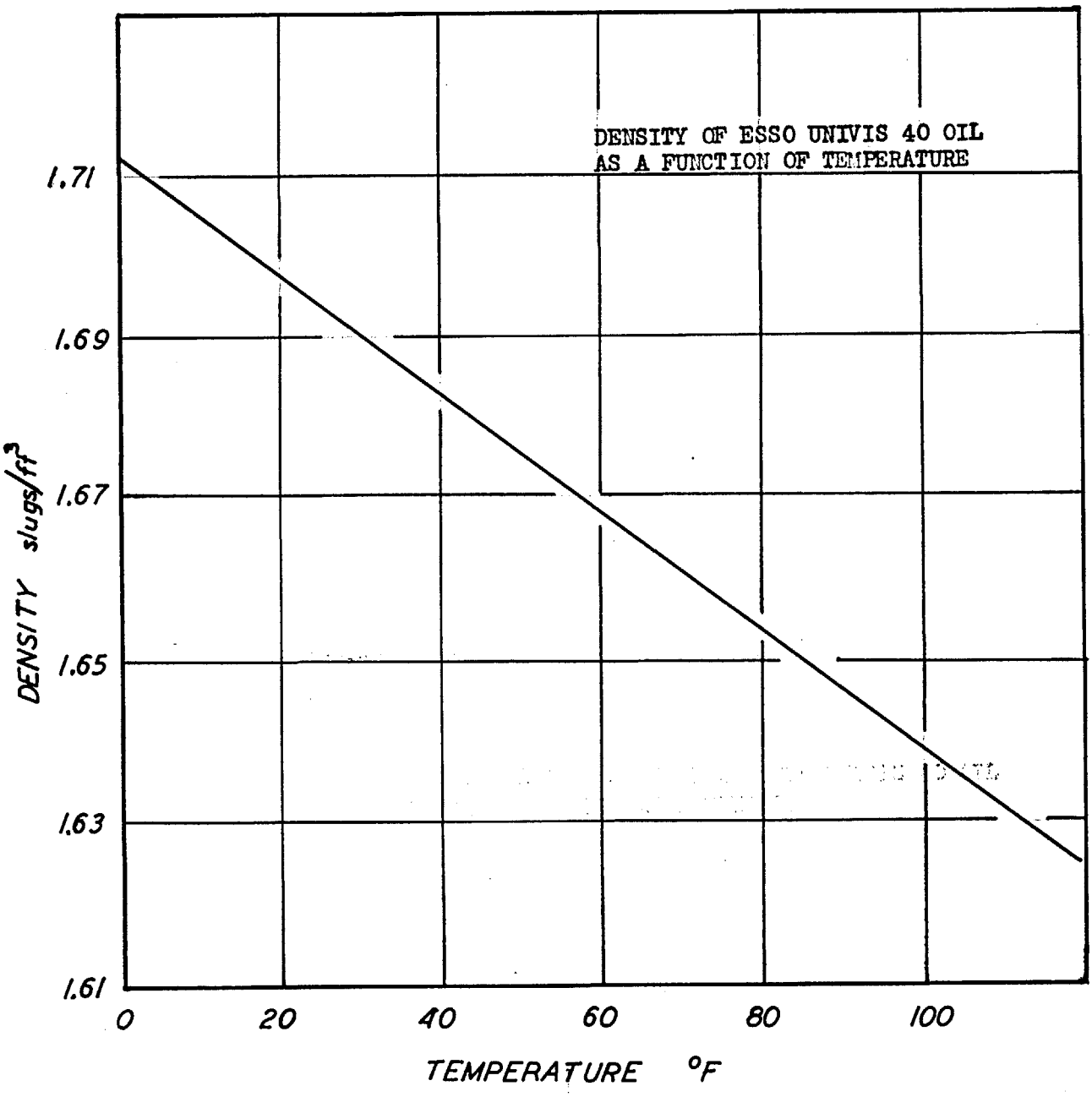
DENSITY OF ESSO UNIVIS 40 OIL
AS A FUNCTION OF TEMPERATURE
1.71
1.69
1.67
1.65
1.63
1.61
DENSITY slugs/ft³
0
20
40
60
80
100
TEMPERATURE °F